

A numerical investigation of the interplay between fireline length, geometry, and rate of spread

J.M. Canfield^{a,*}, R.R. Linn^a, J.A. Sauer^a, M. Finney^b, Jason Forthofer^b

^a Earth and Environmental Sciences Division, Los Alamos National Laboratory, Los Alamos, NM 87545, USA

^b Fire Lab, United States Department of Agriculture, Forest Service, Missoula, MT 59808, USA



ARTICLE INFO

Article history:

Received 12 June 2013

Received in revised form

18 November 2013

Accepted 6 January 2014

Keywords:

Fire

Fireline

Wildfire

Spread

Vorticity

Vortex

ABSTRACT

The current study focuses on coupled dynamics and resultant geometry of fireline segments of various ignition lengths. As an example, for ignition lines of length scales typical for field experiments, fireline curvature is the result of a competition between the head fire and the flanks of the fire. A number of physical features (i.e. buoyancy and wind field divergence for example) arise in and around an incipient fire that defines the shape and spreading pattern of the flame zone. These features are explored using a numerical atmospheric dynamics model HIGRAD, and wildfire combustion physics model FIRETEC. HIGRAD/FIRETEC was designed to investigate wildfires and their interactions with the environment. In this study, the model was used to simulate grass fires that were initiated with a finite length, straight ignition line in homogeneous fuels. The dynamic evolutions of these firelines were analyzed to understand the individual events that evolve a wildfire. By understanding each individual process and how it interacts with other processes, information can be extracted to develop a theory about the mechanisms that combine to produce the observed wildfire behavior. In the current study, the flow field in the region of the simulated fires developed structures consistent with multiple buoyancy-induced vortex pairs. The series of stream-wise vortex pairs produce a regular alternating pattern of up-wash and down-wash zones, which allow air to penetrate the flame zone through troughs created in downwash regions. Consequently, this periodicity in the flow field within the fire resulted in a pattern of residual combustion where prolonged burning occurred in the up-wash zones separated by near-complete fuel depletion in the downwash zones. Some explanation is provided for why increased ignition line length leads to increased rate of spread (ROS) with some asymptotic limit.

Published by Elsevier B.V.

1. Introduction

Today people interact with wildland fires in a variety of ways ranging from evacuation and mitigation, to allowing fires to burn naturally on the landscape, and even setting prescribed fires to manage the forest in order to reduce the danger of wildfires. In all of these interactions and especially in the context of growing populations in forested areas, it is becoming increasingly important to understand wildland fire and improve our ability to predict its behavior.

Fire behavior and its effects are a result of balances between a variety of complex and intertwined processes. The more scientists and practitioners understand about these balances, the better their ability is to anticipate fire behavior. Unfortunately, this understanding is still in its infancy and there is a wide range of phenomena from ignition of individual particles to landscape-scale

coupled-fire/atmosphere interaction that are not well understood. In fact, the most basic roles of radiation and convection in fuel particle ignition and consequent fire spread have not been experimentally investigated (Finney et al., 2013). Developing a better basic understanding of the coupled processes that control wildfire behavior is often difficult when studying wildfires in complex scenarios. Therefore, there is significant value in studying relatively simple fire scenarios such as homogeneous fuels and constant winds.

1.1. Objective

The objective of this paper is to study the factors that connect fireline length, geometry and rate of spread (ROS) for fires originating from line ignitions. This paper is intended to stimulate new perspectives concerning the processes that determine the spread of wind-driven wildfires using coupled fire/atmosphere numerical modeling techniques. To reduce complexity and focus attention on the phenomena associated with the fireline dynamics and geometry, variable environmental conditions that are frequently

* Corresponding author. Tel.: +1 505 665 9118.

E-mail address: jessec@lanl.gov (J.M. Canfield).

found in real-world wildland–fire situations, such as fuel spatial heterogeneity, topographical influences, and wind gustiness, have been omitted. The simulated fires presented here burn through homogeneous representations of tall grass with static prescribed upstream wind profiles at the inlet of the computational domain. The two control variables for this study are ignition-line length and free-stream inlet wind speed.

1.2. Wildfire research tools

Wildfires have been studied using a variety of methods including field observation, laboratory experiment, and numerical modeling. Free-burning wildfires often occur in complex topographic, vegetative, and meteorological conditions and usually occur with no forewarning. Thus, they are difficult to instrument and usually provide only coarse measures of fire behavior. Field experiments can enable more quantitative measurements of these fires, including: ambient atmospheric conditions, fire shape evolution, rate of spread (ROS), and even detailed state and flux quantities at specific points. However, wildfire field experiments are costly, difficult to comprehensively characterize, and are typically performed only under mild fire conditions.

The complexity of wildland fire, the variability of the natural environment, and lack of strict repeatability make it very challenging to completely characterize the conditions that lead to specific wildfire behavior. This makes it even more difficult to broadly diagnose the interplay between the processes at work during a fire.

In order to create a more controlled environment with more repeatability, many researchers such as (Fons, 1946; Dupuy et al., 2011; Finney et al., 2013) have used laboratory experiments to investigate specific aspects of fire behavior. Such experiments can be highly controlled and instrumented with modern techniques in order to test specific hypotheses and to explore assumptions of ignition and spread processes used in modeling. Experimental research has often been focused on determining spread rate for which the scaling to field-scale fires is problematic without the explicit physical processes. Experimental confirmation of physical processes (such as heating, ignition, burning rate, etc.) are essential to understanding how fire spreads and thus, to modeling. Laboratory experimentalists continually work to assess the relevance and context of their work including crucial scaling limitations in order to produce the most meaningful results.

As with many areas of science, impact of these field and laboratory experiments can be increased when they are targeted to address specific hypotheses and when paired with independent and complementary analysis techniques. Numerical models can be used to help in defining or refining such hypotheses in addition to post-experimental analysis of possible interactions between events that lead to specific fire behavior.

In principle, numerical models can provide an additional opportunity to gain perspective on the behavior that is observed in nature and in experiments. The conditions in simulations can be prescribed, altered, and repeated at will, and the effect of different physical assumptions tested. This allows for spatially explicit evolution of dynamic conditions and their relationships to one another to be readily analyzed. Process-based models, for example, are not appropriate for operational use and they are in continual need of validation. However, they can be used to compliment experiments in research applications. Even though such models are not a replacement of real observations, one way to use them is to develop and refine hypotheses that guide experimental designs and eventually assist in the interpretation or analysis of experimental results.

Field-scale observations of wildfires, field experiments and prescribed burns provide researchers with invaluable information that allows both modelers and laboratory experimentalists to

continually assess the context of their efforts and their results. For example, of particular relevance to this study, grass fire experiments were performed and fire behavior data was collected in Australia (Cheney et al., 1993; 1998; Cheney and Gould, 1995). This data has provided a basis for comparison of a variety of model studies including (Linn and Cunningham, 2005; Cunningham and Linn, 2007; Mell et al., 2007; Linn et al., 2012).

Several attempts at computational modeling of wildfires have produced valuable results. However, it is important to keep these works in perspective. The processes that are involved in a wildfire are extremely complex, ranging across chemistry, physics, and biology. Temporal and spatial scales evident in wildfire vary over several orders of magnitude. Any attempt to design a model that represents these processes in a tractable fashion has to make many assumptions to simplify the problem and obtain a solution. The various different models used have a range of approximations and simplifications. Some of these include: WFDS (Mell et al., 2007), FIRESTAR (Larini et al., 1998; Morvan and Dupuy, 2001), HIGRAD/FIRETEC (Linn, 1997; Linn and Harlow, 1998; Reisner et al., 2000; Linn and Cunningham, 2005; Cunningham and Linn, 2007; Linn et al., 2012), and the models proposed by Zhou et al. (2005), Grishin (1997), Séro-Guillaume and Margerit (2002) and Kiefer et al. (2009, 2010). It is critical to state that none of these tools have been fully validated and therefore their results can suggest insights but not be treated as proof.

1.3. Study of wildfire spread

The speed of advancement or ROS of a fire in the direction of the wind is a result of the interaction between a variety of processes including heat transfer, moisture evaporation, fuel ignition, and combustion rates. One of the best-known relationships between fire and the environment is the positive correlation of ROS in the direction of the local wind and the wind speed. This has been shown in the laboratory (Carrier et al., 1991; Wolff et al., 1991; Weise, 1993; Catchpole et al., 1998) and in the field (Cheney et al., 1993, 1998; Cheney and Gould, 1995).

One-dimensional theoretical models were previously developed based on perceived physical relationships (Pagni and Peterson, 1973; Koo et al., 1997). In other scenarios, empirical models and physical principals were combined to model fire behavior in a one-dimensional context that utilized the relationships between wind, ROS, and topographic slope (Rothermel, 1972; Cheney et al., 1998; Dupuy and Larini, 1999). These simplified models have provided impressive results in some wildfire contexts (e.g. Rothermel, 1972). Some of these models were developed further into two-dimensional horizontal planar models producing estimates of the evolution of complex fire perimeters, such as FARSITE (Finney, 1998) and the model developed by Margerit and Séro-Guillaume (2002). These models have produced realistic results in some scenarios, but they are not appropriate for explaining interplay between individual physical processes or introducing general hypotheses regarding cause and effect relationships.

A variety of factors affect fireline dynamics, including fuel bed conditions and atmospheric conditions. Primary in its affect on the dynamics of a fireline including its ROS is local wind speed. Yet, this fundamental dependence is not fully understood (Baines, 1990; Beer, 1991, 1993; Linn and Cunningham, 2005; Cunningham and Linn, 2007).

In grassfire experiments (Cheney et al., 1993, 1998; Cheney and Gould, 1995), laboratory experiments (Finney et al., 2013) and recent numerical grass fire studies using physics-based models (Linn and Cunningham, 2005; Cunningham and Linn, 2007; Mell et al., 2007), free-burning fires were observed to have both fireline-scale curvature and finer-scale heterogeneity along the fireline. However, the ways that these facets of fireline structure might

Table 1
Simulation parameters.

Simulation name	Domain dimension ($X \times Y \times Z$ m)	Ignition line length (m)	Ambient wind speed (m s^{-1})
U03L20	$960 \times 240 \times 615$	20	3
U03L100	$960 \times 320 \times 615$	100	3
U03L200	$960 \times 420 \times 615$	200	3
U03L400	$960 \times 640 \times 615$	400	3
U06L20	$960 \times 240 \times 615$	20	6
U06L100	$960 \times 320 \times 615$	100	6
U06L200	$960 \times 420 \times 615$	200	6
U06L400	$960 \times 640 \times 615$	400	6

be related and their combined effects on fire spread has not been explained. Cunningham and Linn (2007) described the simulated evolution of the local heat transfer mechanisms and the turbulent coupled atmosphere–fire interactions at various locations along a fireline with different orientations with respect to the wind (i.e. forward and lateral spreading portions of the fire). However, this previous work was not able to comment on the importance or impact of fireline curvature or the reason why length of fireline impacted the spread rate as noted by previous researchers (Cheney et al., 1998; Mell et al., 2007).

2. Methods and strategy

This study used the numerical wildfire model, FIRETEC (Linn, 1997; Linn and Harlow, 1998), which attempts to represent multi-phase chemistry and physics in a bulk sense by resolving quantities at approximately meter-scales. FIRETEC is coupled to a fully compressible, non-hydrostatic, atmospheric-dynamics model, HIGRAD (Reisner et al., 2000) specifically designed to operate at higher resolution compared to traditional mesoscale models.

A total of eight simulations were performed for this study. They were all identical in resolution, with 2 m resolution in the horizontal directions and ~1.5 m near the ground. The vertical dimension of the computational cells increases with height above the ground. The domain dimensions were all 960 m stream-wise (x-direction) and 615 m in the vertical dimensions (z-direction). These simulations differed in the cross-stream (y-direction) domain dimensions from 240 m up to 640 m, based on the length of the ignition line. The ignition line lengths were respectively 20 m, 100 m, 200 m, and 400 m. The cross-stream width of the domain was set such that on either side of the ignition line, 110 meters of space resided between the y-boundaries and the initial fireline. The 400 m cases differed in that 120 m of space resided between the ends of the ignition lines and the y-boundaries. These distances were chosen as a balance between computational efficiency and placing the computational boundaries far enough from the fireline as to limit their effects on the fireline dynamics and fire-induced flow field. These domain parameters are summarized in Table 1.

In order to study the influence of the fireline on the wind field around it, the complexity of a realistic, dynamic, turbulent wind field was omitted (i.e. flow conditions are restricted to a low Reynolds number regime for atmospheric flows). The initial and upstream winds were specified using exponential decay profiles (Linn et al., 2012) (Fig. 1). They reach a wind speed of 3 and 6 m s^{-1} at ~50 m and above. These profiles set the inlet boundary condition, 100 m upstream of the ignition lines. The inlet flow field was laminar. Turbulent fluctuations of length scales greater than 2 m, which would be present in field observations, were omitted in order to isolate the mean flow affects on the fireline. Since these are large eddy simulations (LES), there is unresolved turbulent kinetic energy associated with the sub-grid resolution scales. Thus, the energy

associated with meter-scale and smaller velocity fluctuations was represented in the inlet flow field through the turbulence closure scheme.

The simulated propagation distance is considered to be the farthest downwind distance from the ignition line at a given time where fuels have reached or exceeded a solid temperature of 500 K. Average ROS values are determined by the slope of the linear least squares fit to the propagation distance versus time curves after the initial acceleration phase.

Trends in Cheney et al. (1993), Mell et al. (2007) and Linn and Cunningham (2005) suggest the sensitivity of ROS to ignition line length diminishes with increasing length. However, these previous studies have included a more limited range of fireline lengths than the current study. With nearly four times the range of fireline lengths, this study supports comprehensively their results of diminishing effects of line length. Functional forms of the spread rate vs. fireline length (L) can be hypothesized based on the ROS trends with line length. Cheney and Gould (1995) proposed a functional form of this dependence as:

$$R_{\text{OS}} = A(1 - e^{-bL}) \quad (1)$$

With the assumption that there is some asymptotic limit to the ROS, as the crosswind expanse of the fireline, L , increases, it is also reasonable to postulate the functional form:

$$R_{\text{OS}} = A \cdot \tanh(bL) \quad (2)$$

In Eqs. (1) and (2), A is a scaling coefficient with units of m s^{-1} , and b is a length scale with units of m^{-1} . The coefficient, A , can be interpreted as the theoretical “quasi-steady” ROS when fireline width approaches infinity (R_{∞}).

Another diagnostic variable that is examined in this study is helicity. Helicity is a measure of the magnitude of flow rotation about an axis aligned with the local instantaneous flow velocity, V . Helicity, H , is the dot product of velocity and vorticity:

$$H = V \cdot \nabla \times V \quad (3)$$

The flow characteristic described in (3) was extracted while post-processing the simulations. It was a useful diagnostic for helical motion in the flow-field near the fireline and is discussed in the results section.

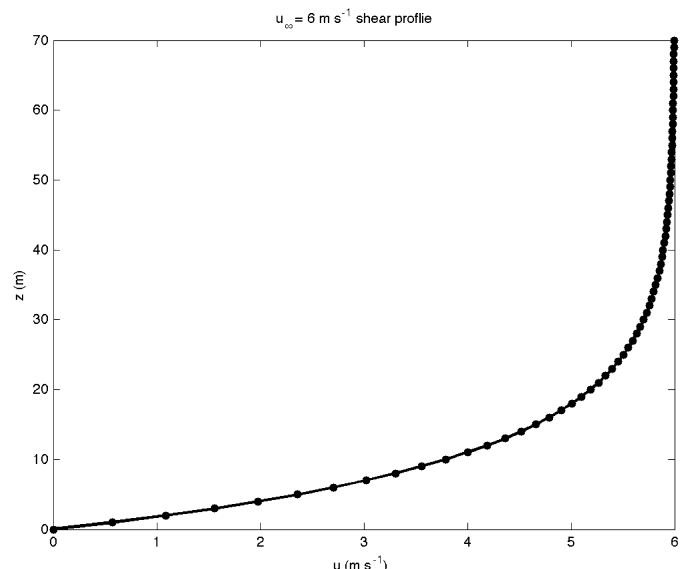


Fig. 1. Initial and boundary condition wind profile for the U06 cases. The U03 cases have the same profile, but they are scaled to 3 m s^{-1} .

3. Results and discussion

3.1. Fireline geometry trends

Fire simulations with various ignition lengths displayed both similarities and noticeable differences in fire behavior (Fig. 2). All of the firelines become curved in nature with the heading portion of the fireline, roughly the central region of the fire, spreading at a faster rate than the ends of the fireline. In these simulations, which omit resolved cross-stream wind fluctuations at the upwind inlet of the domain, the 20 m firelines show minimal development or extension of flanking fires near the ends of the fireline where as the 100-m and longer firelines show significant development of flanking portions of the fireline. This is consistent with results shown by Linn and Cunningham (2005). Spread of the fire in the cross-stream direction was observed in the 100-m and longer ignition lines. However, it is important to note that even with FIRETEC's probability distribution treatment for sub-grid temperature variations, the 2-m horizontal resolution of these simulations might preclude adequate representation of flanking fire that are extremely thin and propagate by connectivity of the fuel matrix. This is under investigation through separate efforts.

In Cheney et al. (1993) grassfire observations found two typical fire shapes. The first was a broad, parabolic-shaped headfire in which the flanks develop to a width that is greater than the ignition line, a characteristic that was present in the simulations of larger fires. The second was a narrow pointed headfire, where the width did not exceed the original ignition line width, resembling the simulated fires with shorter ignition lines. The degree of lateral spread in the simulations is expected to potentially increase under more realistic fluctuating wind conditions, but this element of wind–fire interaction is outside the scope of this manuscript.

In this suite of numerical simulations under idealized winds, the magnitude of ambient wind (3 or 6 m s^{-1}) did not significantly change general geometric trends toward these two fire shapes given initial line width. Simulated fireline behavior was also consistent with the previous effort of Linn et al. (2012), where the longer firelines show significant stream-wise heterogeneity along the heading portion of the firelines, including prominent fingering structures upwind of the headfire.

3.2. Rate of spread

ROS for the simulated grass fires increase with fireline length, which is consistent with observed trends in (Cheney et al., 1993) and previous numerical findings (Mell et al., 2007; Linn and Cunningham, 2005). For the ignition-line lengths of 100 m and greater and wind speeds of 3 m s^{-1} the propagation curves in Fig. 3a and b continue to increase in slope until around 350 s, whereas the U03L20 and 6 m s^{-1} simulations become nearly linear by 150 s. This adjustment period correlates with the fireline transitioning from the straight ignition line to a curved fireline with stream-wise finger structures upwind of the headfire. After this period the fireline reaches a balance and the spread rate approaches a linear relationship between time and propagation distance. Cheney and Gould (1995) called this the “quasi-steady” rate of spread. Although the qualitative trends in ROS with fireline length are consistent with Cheney et al. (1993) observations, it is not meaningful to directly compare the ROS values from these idealized numerical simulations to these field observations due to the fact that the fuels are different, the incoming mean wind profiles are different and these simulations purposely omitted the natural fluctuations in the wind, which are always present to some degree in a natural environment. The average ROS values are given in Table 2.

Table 3 shows the coefficient values resulting from the non-linear curve fits to Eqs. (1) and (2). Fig. 3c illustrates these functional

Table 2
ROS for each case.

Wind speed $U_{10\text{m}}$ (m s^{-1})	Ignition line			
	20 m	100 m	200 m	400 m
3.00	0.20	0.68	1.10	1.15
6.00	0.27	1.19	1.45	1.75

relationships plotted with the ROS from the simulations. The values of coefficient A, derived from the curve fitting of Eqs. (1) and (2) compare favorably to the range of ROS values for the infinite line simulations in Linn et al. (2012) as shown in Table 3.

The coefficients presented in Cheney et al. (1998) show a stronger ROS dependence on line length than values obtained under the present simulations. These differences between the empirically-derived relationship and those produced by the simulations could be due to disparities between actual and simulated environmental conditions, such as fuel bed characteristics, or upstream atmospheric conditions including wind shear, wind variations or turbulence. Under the parameter range of scenarios performed here, we can only hypothesize about the functional form and the values of coefficients. Determining the sensitivity of these coefficients to various fire conditions is outside of the scope of this work. But, further investigation in conjunction with laboratory and field observations into this notion would be enlightening. By explaining empirically measured trends a future study might also have some relevance to understanding the changes in fire behavior when long firelines become broken into separate segments by natural or anthropogenic means.

3.3. Fire shape

One distinct feature that appears in all of the simulated fires in which width ignitions were greater than 20 m in length is cross-stream fingering of the fireline upstream of the headfire (Fig. 2). Such cross-stream fingering in the post-headfire fuel has been noted in past modeling exercises (Linn and Cunningham, 2005; Kiefer et al., 2010; Linn et al., 2012). Kiefer et al. (2010) found that convective rolls aligned with the mean flow, are prevalent near the ground. There have also been indicators of such structures in field conditions (Fig. 4) and laboratory fires (Fig. 5) (Finney et al., 2013).

The fingering of residual combustion behind the flame front occurs because of the development of longitudinal counter-rotating vortices (Linn et al., 2012), which are similar to flow structures in numerous boundary layer flow scenarios. Such vortices, illustrated for the U06L400 simulation (Fig. 6), are remarkably similar to those developing from Taylor–Görtler instabilities that develop in boundary layer flows (Floryan, 1991). Classical Görtler vortices result from impingement of fluid onto a curved surface with uniform elevation over the cross-stream dimension. Studies of heated boundary layer transition to turbulence (Sparrow and Husar, 1969; Maughan and Incropera, 1987) have shown that Görtler-like structures are initiated by the interactions between stream-wise inertial flows and buoyancy-induced vertical flows. This has been shown in a number of laboratory, numerical, and theoretical studies (Kuo, 1963;

Table 3
Curve fits for ROS vs. fire line length.

Wind speed (m s^{-1})	Curve-fit equation from Section 2	A (m s^{-1})	b (m^{-1})	R_∞ (m s^{-1}) (Linn et al., 2012)
3	1	1.22	9.19×10^{-3}	1.14–1.35
6	1	1.75	10.2×10^{-3}	1.91–2.27
3	2	1.18	7.09×10^{-3}	1.14–1.35
6	2	1.69	8.13×10^{-3}	1.91–2.27

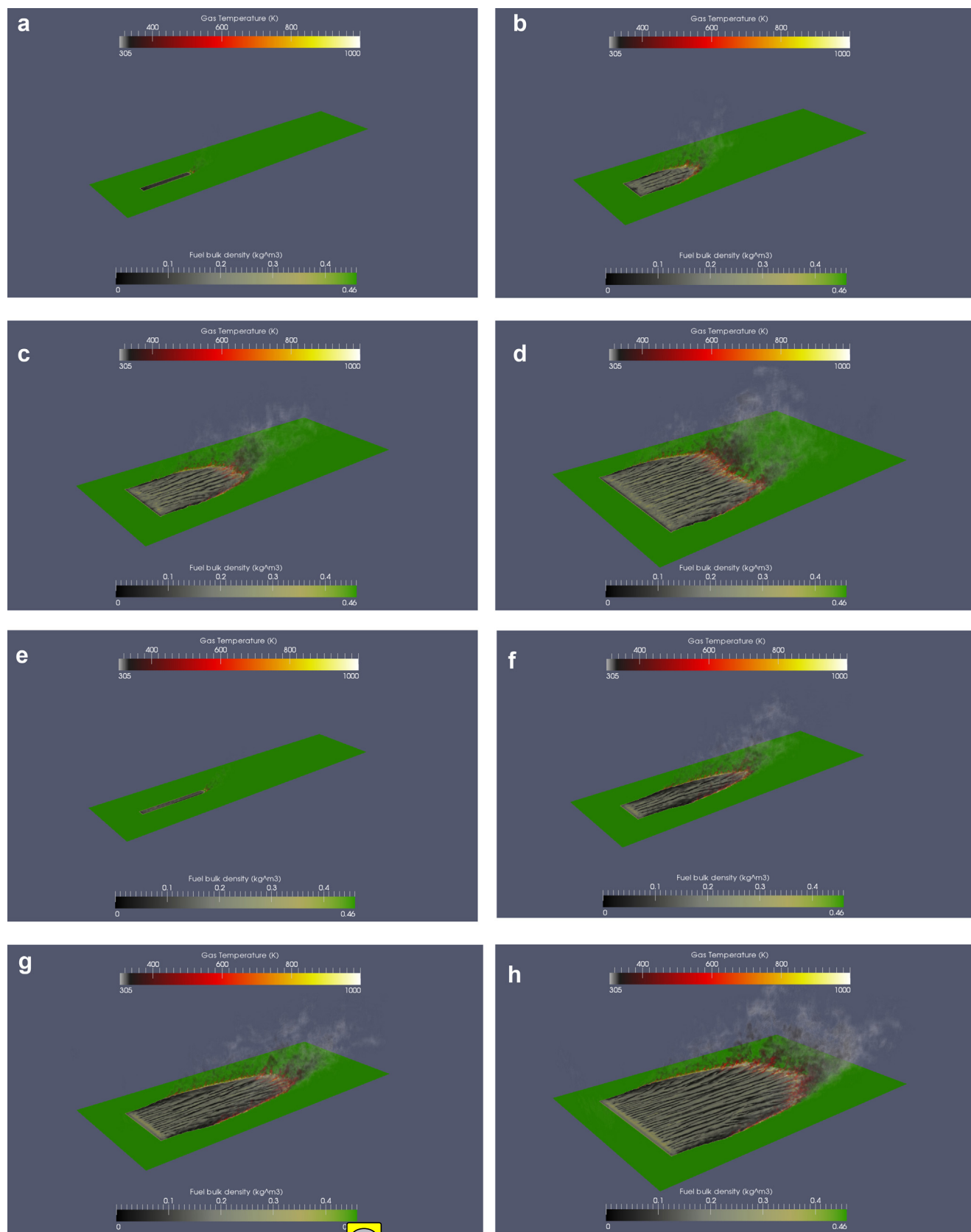


Fig. 2. Each scenario after 400 s of simulated time. The left column contains the 3 m s^{-1} simulations and the right column shows the 6 m s^{-1} simulations. Gas temperature is volume rendered with fuel bulk density contoured beneath it.

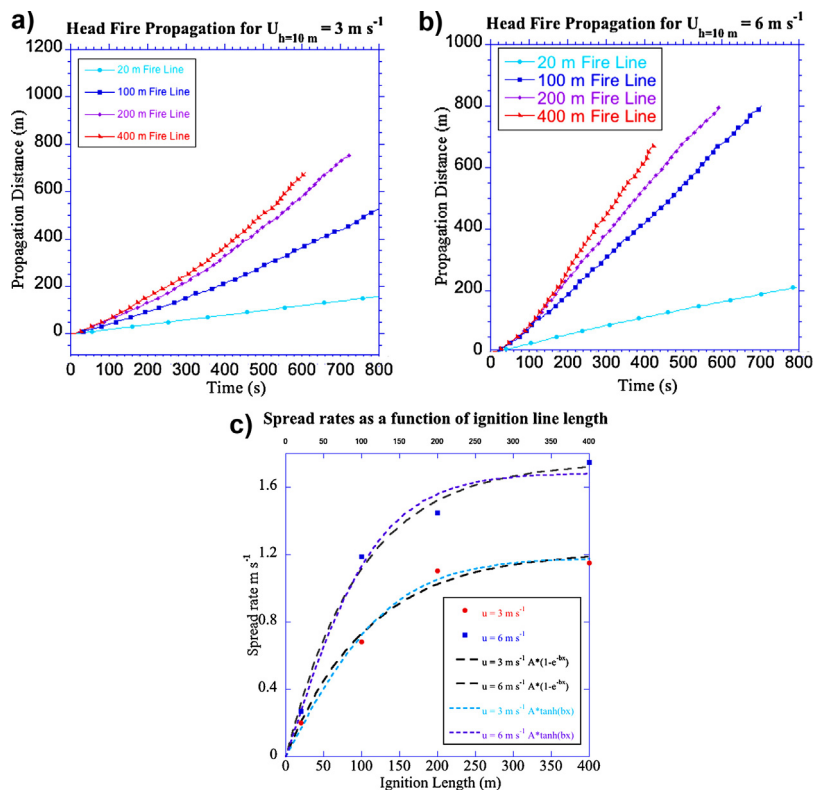


Fig. 3. (a and b) Fire propagation distance plotted against time for each set of wind speeds and (c) spread rates as a function of ignition length.

Deardorff, 1965; Gage and Reid, 1968; Asai, 1970; Clever and Busse, 1991, 1992). The similarity of the two vortical structures comes from the analogy that the curved surface induces velocity components normal to the inertial paths of the fluid much like buoyancy forces do. The thermally driven vortices observed upstream of a fireline are concurrent with a buoyancy field that has variation over the cross-stream direction. In this case, air penetrates through the buoyant rising gasses in places as apposed to impinging onto any surface. The convergence between pairs of these vortices produces alternating patterns of up-wash (away from the surface) and down-wash (toward the surface) in the flow field. In the context of fires, oxygen-rich air is drawn toward the surface in a down-wash where it diverges and is driven laterally into the burning

regions, then subsequently heated and evacuated vertically in the up-wash.

The thermally driven vortices observed upstream of a fire are further accentuated compared to those of a uniformly heated boundary layer. This is so because their presence drives cross-stream heterogeneity in the combustion and temperature fields with hotter locations in the up-wash zones and cooler areas under the down-wash areas. In the up-wash zone in a fire context, the convergence of oxygen and pyrolyzates, increases mixing and vertical acceleration of the gases producing taller flames. Hence, a regular pattern of flame towers and troughs along the fire edge are observed. As they increase in length, the vortices display secondary sinuous or varicose instabilities causing them to sway laterally as observed by Floryan (1991) and by Clever and Busse (1992). These vortices merge down-stream of their initiation such that the span-wise wavelength increases. Intense burning in the up-wash zones, makes for an oxygen poor, yet fuel-rich environment that limits the burning rate of solid fuels and enables the prolonged burning visible as residual fingers of burning behind the fire front (Figs. 2, 4 and 5).

Fig. 6 is a plot of helicity above the fire. It shows the tightly connected, uplifting vortex pairs aligned with the fuel scars. Regions of maximum solid temperature, fuel consumption, and vorticity gradient are collocated at the surface. Fig. 6 shows alternating regions of positive and negative helicity (green and blue, respectively). The tight seams between the green and blue regions of helicity are the areas where flow is rising behind the fireline (up-wash). The larger gaps between the vortex pairs are areas where cool air is being drawn down to the surface (down-wash). In the regions of uplifting vortex pairs, mixing-limited combustion enables the fuel to burn for an extended time and provides an elongated buoyancy source behind the fire front, further driving the counter-rotating vortical structures.

As the fire heats the air, leading to buoyant plume rise, a pressure deficit is formed underneath the rising column. In order to fill the void left by the rising air, the local wind field adjusts and



Fig. 4. Photograph of a large grass fire in Australia near Burrinjuck Dam. Commander Chris Hadfield took this image from the International Space Station on January 9, 2013. The longitudinal smoke streaks are consistent with patterns of residual combustion associated with the fingering of simulated grass fires.

Photos courtesy of the Fire Lab, USDA Forest Service.

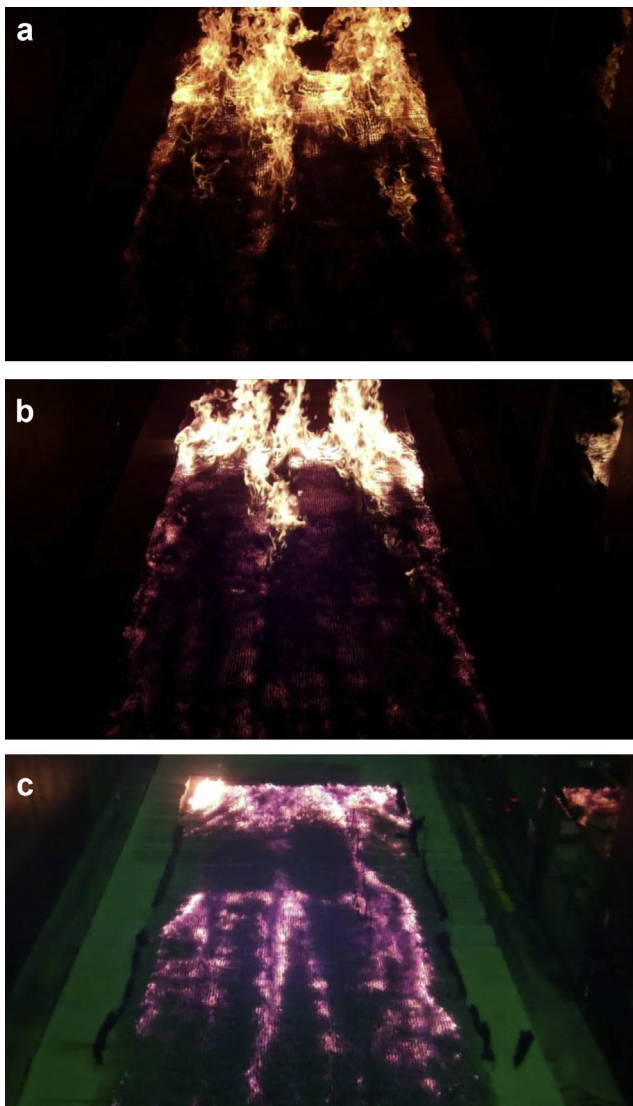


Fig. 5. Views downwind of an experimental fire burning in cardboard fuel beds shows a sequence of fire movement leaving fingers of burning fuel. Notice that the taller flame peaks are associated with residual combustion behind the fireline. Photos courtesy of the Fire Lab, USDA Forest Service.

in-drafts form toward the base of the fire. The combination of the rising motion and the draw of air to the base of the fire cause intense mixing and accentuate the rotation in the vortex pairs.

Fig. 6 shows that the black fuel streaks adjacent to the flanking fires curve toward the fireline at their termination points. The turning of these streaks indicates a redirection of the flow upstream of the fireline to accommodate the in-drafts of the flanking section of the fireline. Such fuel consumption features might be of use in the field as a forensic tool to understand how fire burns through vegetation. The curvature in fuel consumption patterns may indicate the difference between mean ambient flow and the winds being significantly influenced by the in-draft of the flanking fire.

In the eight scenarios of this investigation the separation distance between the fingers of heavily depleted fuel is similar near the ignition line for all scenarios and showed no significant dependence on initial line length. In firelines with the highest quasi-steady ROS, such as U06L400, a few of the fingers merge together as they move downstream (Fig. 6). This occurs more often in the longer fireline and faster wind speed simulations than those with shorter firelines or weaker wind speeds even though the spatial frequency

of the fingers near the ignition line is similar between the various cases. This merging is indicative of small vortical structures compounding to form larger ones. Laboratory experiments (Finney et al., 2013) have suggested that the size of these vortical structures or their cross-stream separation distance grows as the depth of the fireline increases. Both simulations and experiments illustrate that the depth of the fireline is greater after the fires have accelerated to a quasi-steady state than they were at the time of ignition. Since the fireline depth increases as the fire grows, it follows that the number of fingers would also evolve with the fire and hence the length-scale of vortices. In some of the cases, when the gap between two fingers becomes large enough, a new finger starts. The length scales determining the size and cross-stream frequency of these counter-rotating pairs and the corresponding fingers were previously suggested to be functions of ambient wind speed and fuel load in Linn et al. (2012). These simulations suggest that a correlation between wind speed and frequency for the counter-rotating pairs may be tied to the length of the heated zone upwind of the fire front, which stretches out as fireline depth gets larger for faster moving fires. Increased fuel load would change the near-surface drag, slow the fire spread and potentially increase the local buoyant source. Future laboratory and simulation-based research will provide additional information, concerning these relationships.

3.4. Pressure gradient influences

In wind driven fire scenarios, the buoyant column of rising air can partially obstruct the ambient flow, with the obstruction effects increasing as the strength of the buoyancy (correlated with fire intensity) increases relative to the strength of the ambient wind. As with other flow obstructions, a low-pressure region forms on the downwind side of the fire and plume (Fig. 7). It is reasonable to expect a macro-scale negative pressure gradient from the upwind side of the fire to the downwind side of the fire. The wake-like region of reduced pressure downstream of the fire serves to redirect the ambient winds, in effect pulling air around the flanks as suggested in Cunningham and Linn (2007), but can also incite flow through the fireline. In the conceptual infinite fireline scenarios of Linn et al. (2012), winds were not able to circulate around the fireline, instead air could only be pulled into the downstream lower pressure region through the flaming front.

The macro-scale pressure gradient across the fireline is greatest at the head of the fire and tapers off as the fireline curves around into the flank. The small-scale pressure perturbations within the fireline are extremely complex and not a facet of this study. However, the fireline-scale pressure field consists of a macro-scale pressure gradient across the fireline (highlighted in Fig. 7a and b) that directs the ambient flow field.

Results of these numerical simulations suggest that a longer fireline will tend to allow more wind to push through it, in contrast to a shorter fireline where the winds can be redirected more efficiently around the fire rather than through it (see Fig. 9). The penetration of winds through a fireline along the troughs created by downward motion from the vortices, forces hot gases forward into unburned fuel, allowing the flames to impinge on fuels downstream of the active combustion zone. This notion is consistent with the evidence that increasing fireline width is correlated to increased ROS. In all of the simulated fires, air circulates around the outside of the fireline and is pulled into the low-pressure region downstream of the fire. However, even in the 400-m fires, the ability for the air to circulate around the fire and reduce the pressure deficit behind the fire should be recognized as a difference from the infinite length firelines (Linn et al., 2012) where there is no recirculation around the edges. The similarity of the shape of streamlines outside of the flanking portions of the various fires, such as those shown in Fig. 7, suggest that either the presence of the boundary over 100 m away

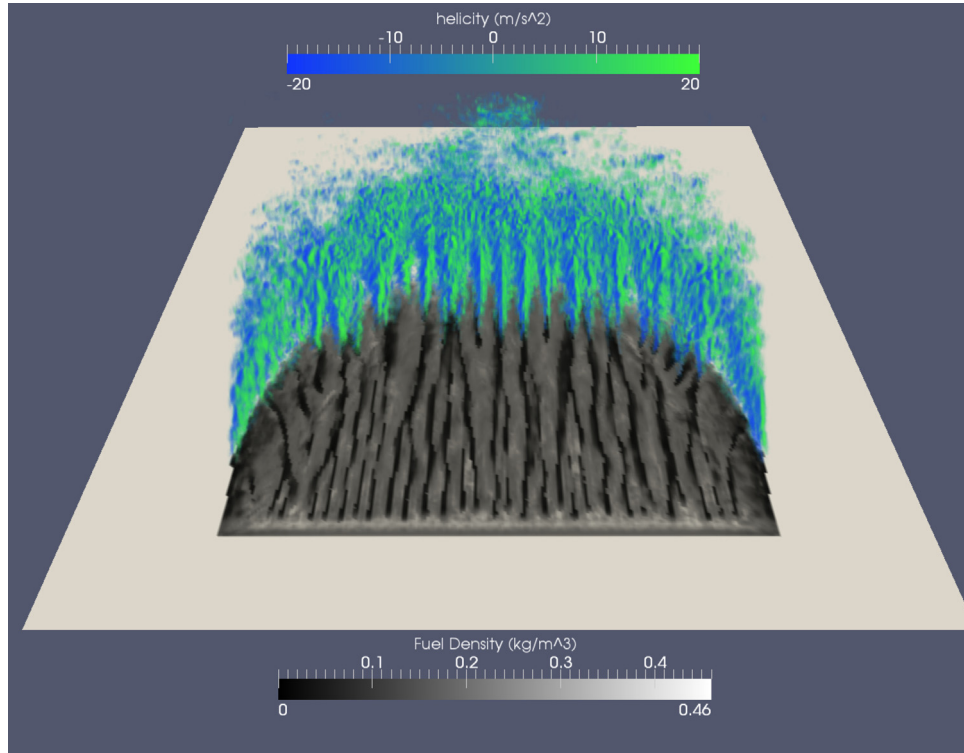


Fig. 6. Isosurfaces of helicity in the vicinity of the fireline for the U06L400 case.

from the fireline has limited impacts on the fire behavior or at least that the effect was similar for the different widths of fires.

3.5. Streamlines and fireline shape

Streamlines are frequently used in the context of steady-state flow fields to illustrate salient characteristics of flow patterns. In complex and dynamic flow fields such as those related to wildfires, streamlines in an instantaneous snapshot of the flow do not exactly convey the path that a parcel of air would travel since the downstream patterns are always changing. This caveat is especially important when considering a parcel of air that is near the actively burning fireline. For similar reasons, streamlines are less meaningful in high turbulence areas, such as the region directly downstream of the fire. However, in situations where the upstream features are only slowly evolving compared to the speed of the flow, streamlines can be used to observe quasi-steady flow patterns such as those farther upstream of a fire. With this in mind, Figs. 7 and 8 show streamline representations of the far-field (away from the fireline).

The horizontal flow patterns upstream and to the sides of the fires are depicted with the use of streamlines in Fig. 8a and b. These streamlines are initiated in the computational plane nearest to the ground at the upstream boundary of the domain and can be interpreted as paths that air parcels follow toward the fire if they enter the domain in this region. In two dimensional flow fields, divergence of streamlines indicates that the flow is slowing down. However, in this three dimensional flow field, divergence of streamlines indicate that air is entering the plane of interest from above or below and the termination of a streamline indicates that a parcel on this trajectory is exiting the horizontal plane of interest. In Fig. 8a and b, the curving of the streamlines as they approach the fireline, is a redirection of the ambient flow field to meet the

in-draft needs in the fireline. Fig. 8a and b shows that regions of streamline divergence are correlated to downdrafts.

In Fig. 9, an idealized diagram of a short and long fireline is presented. In both images, the thick dash-dot line represents the fireline, the curved arrows give the flow direction, and a cloud depicts an air parcel with a number in it. The numbers represent sequential times. The air parcel in Fig. 9a starts upstream of the fire at time 1. At time 2, it is split into two parcels due to the competition of the two flanks. At time 3, each of the parcels has been pulled toward one of the flanks. In Fig. 9b, the fireline is longer and the flanks are farther apart. At time 1, the parcels are upstream of the fire. At time 2, the parcels have been deflected slightly in the direction of the closest flank, or in the case of the middle parcel, it has been pulled toward the fire head. At time 3, each of the parcels is near one of the flanks or the head. Note that in Fig. 9a, the initial parcel was pulled apart by the in-drafts at either flank, while in Fig. 9b, the air parcels were only translated and not pulled apart.

In the U06L100 case depicted in Figs. 8a and 9a, competition between the in-drafts of flanking and heading portions of the fire results in the headfire being driven forward by a lower integrated volume of air than observed in the U06L400 case (Figs. 8b and 9b). This headfire-flank competition for air diminishes as ignition length increases, due to the relative abundance of air upstream of the fireline. This trend was observed in all of the simulated fires and resulted in lower ROS for the shorter ignition line cases. Figs. 8a and 9a demonstrates this, where most of the streamlines are diverted to the flanking in-drafts before they reach the head fire, while Figs. 8b and 9b shows that many of the streamlines are unaltered and proceed directly toward the headfire.

The competition between the head fire and the flanks of the fire result in narrow, sharply curved, firelines for short ignition lines (Figs. 8a and 9a). The broader, more gradual curvature originates from long ignition lines (Figs. 8b and 9b). As air approaches the

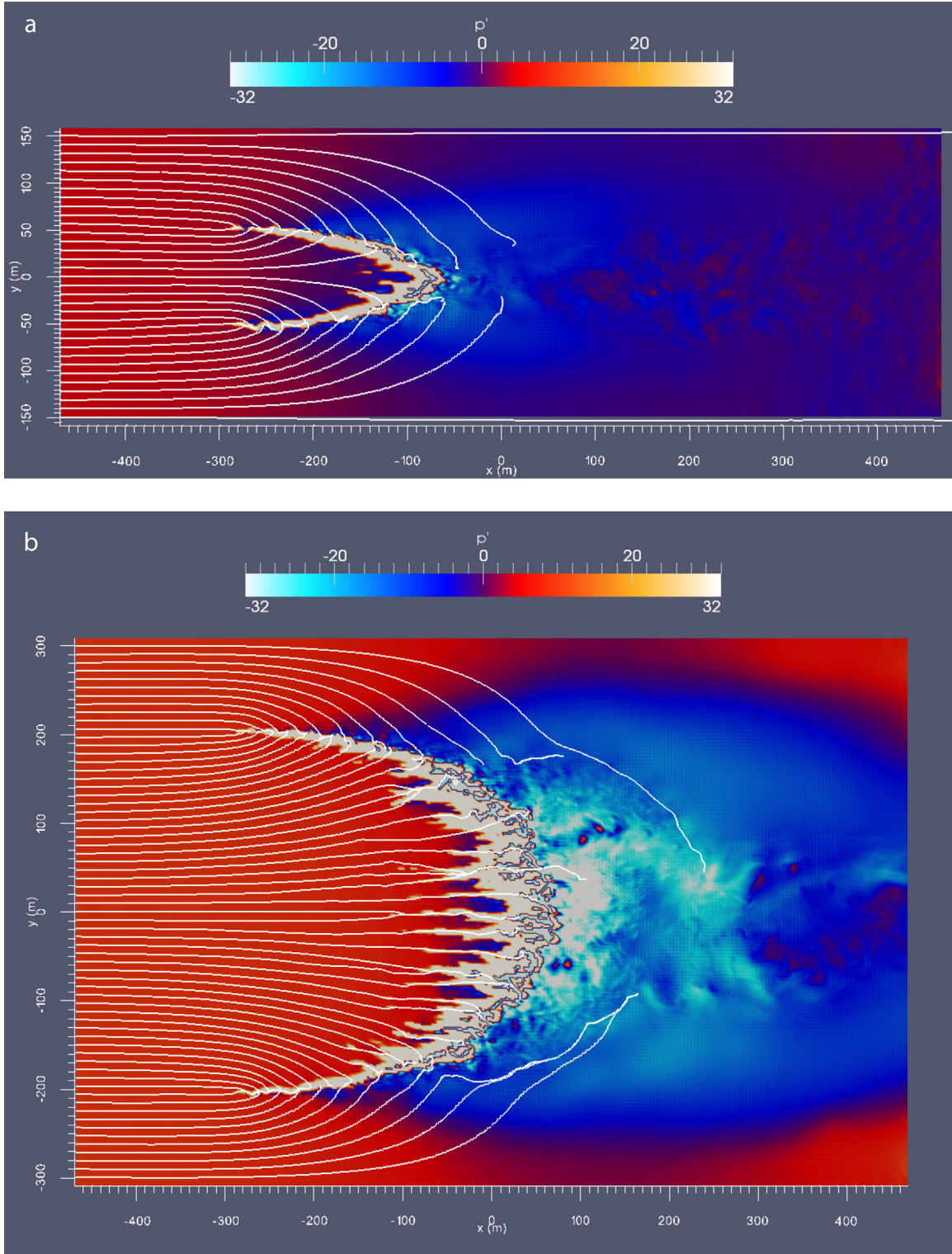


Fig. 7. (a) Pressure perturbation from the mean for the U06L100 scenario with streamlines. (b) Pressure perturbation from the mean for the U06L400 scenario with streamlines.

fireline from the upwind direction (Fig. 9a and b) it pulls air toward the “flank” or “head” section of the fireline via buoyantly driven in-drafts and mass conservation. When the fireline is curved, there can be multiple parts of the fireline where in-drafts are competing for the same parcel of upstream air. When the flanking portion of the fireline competes with the headfire, less stream-wise moving air reaches it (Figs. 8a and 9a). In this case the headfire feels

an effectively reduced local wind speed compared to a scenario with no nearby flanking fire as seen in the longer ignition cases (Figs. 8b and 9b).

Based on the flow and burn patterns of simulations here, one hypothesis for future work is that the rate of lateral spread of a fire is also affected by the length of the fireline. The competition between flanking sections combined with the in-draft needs of the

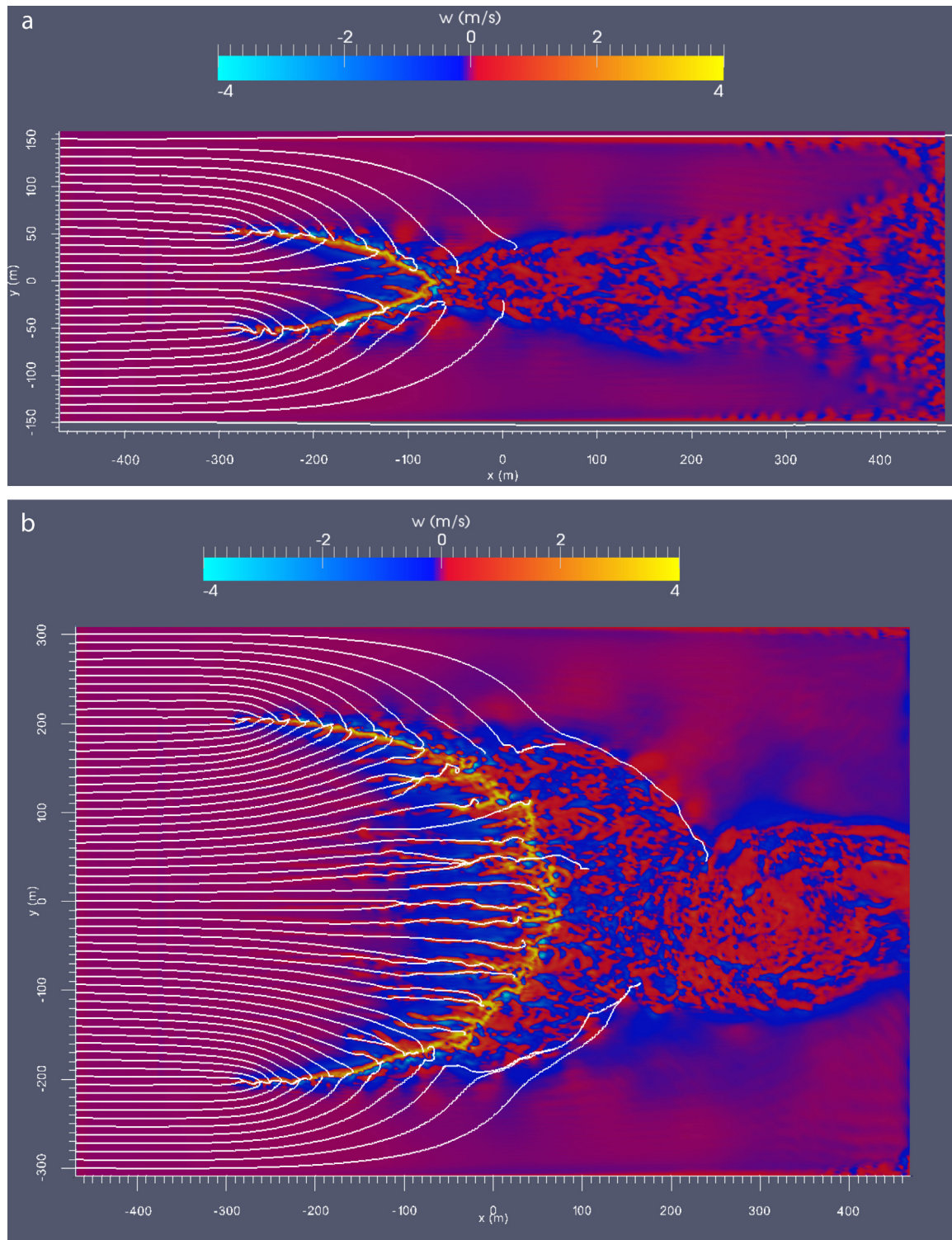


Fig. 8. Vertical velocity color contours with streamlines for (a) U06L100 and (b) U06L400.

head fire shift the balance of incident wind such that the quantity of wind coming from upstream to the inside of the fireline increases for longer firelines, effectively increasing the net draw from the outside of the flank. In flanking regions, spread to unburned fuels (i.e. lateral spread), is much more sensitive to the local radiative and convective heat transfer balances since lateral spread is (at least

here) perpendicular to the ambient winds. This relationship between lateral spread and distance between fireline flanks is likely a function of burning zone dimensions. In thin burning zones, such as might occur with lighter fuel loads, the in-drafts would be reduced and it would be easier for flanking fires to sustain themselves. Also, with higher ambient winds, the supply of air from the

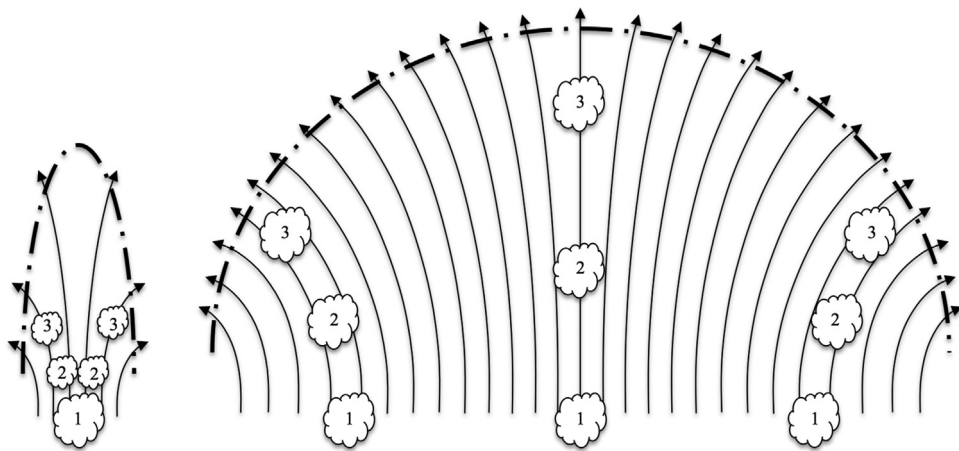


Fig. 9. Diagram illustrating the idealized paths that air parcels (cloudy shapes) follow as they approach a curved fireline. The dot-dashed bold line represents the fireline location and the curved arrows dictate the path of an air parcel. The air parcel travels sequentially as shown by the numbers: (a) short ignition line and (b) long ignition line.

mean atmospheric flow is increased and thus the draw between the flanking fire lines would be diminished.

4. Conclusions

In the numerical simulations performed here using HIGRAD/FIRETEC, relationships between fireline shape, fire induced in-drafts, fireline-scale pressure gradients and rate of spread have been examined. The simulations incorporated simplifications from realistic scenarios including: a homogeneous upstream wind field, which lacked resolved turbulence or cross-stream directional shifts at the upwind boundary of the domain; homogeneous grass fuels, where local variations in fuel density, height or moisture content have been ignored. The results of these simulations provide support for previous hypotheses, a basis for new hypotheses and additional perspectives regarding field observations.

The simulations of this study included ignition lines ranging from 20 to 400 m in length and two different wind speeds. As expected, based on previous field observations and numerical studies, the simulations showed increasing headfire ROS with length of ignition line for both tested wind speeds, but over a much larger range of ignition line lengths than previous studies. In addition, these simulations also showed a dependence of flanking fire behavior on ignition line length.

This study suggests that the fire-induced in-drafts along the flanks of a fireline compete with those of nearby portions of the headfire for the upstream winds, thus steering some of the incident wind away from the headfire. This competition serves to slow down ROS of the nearby portions of the head fire and contributes to the curvature of the headfire. In the longer ignition line scenarios, more of the upstream wind reaches the headfire, enhancing the wind penetration through the fireline and also the heat transfer downstream to unburned fuel. As headfire width increases the competition between flanks and head fire for upstream in-drafted air is reduced, allowing flanks to more effectively divert incoming air. As a result the net flow across the flank sections of the fireline can be stronger toward the unburned fuel, increasing the ability for the fire to spread laterally.

The numerical results of this study also suggest the presence of a fireline-scale negative pressure gradient from upwind of the fireline to downwind of the fireline. This pressure gradient contributes to the penetration of wind through the fireline and resultant convective heating of unburned fuel leading to increased ROS. The magnitude and effectiveness of the pressure gradient in increasing

the ROS is dependent on the length of the fireline. The magnitude of the effective pressure gradient across the fireline is influenced by the upstream in-draft competition between flanking and head fires.

These simulations did not explore the effects of resolved ambient cross-stream variability in winds, nor the effects of the fundamental fuel characteristics of bulk density, moisture content, surface area to volume ratio, and fuel bed height on fireline shape and ROS (forward or lateral). Conclusive explanation of the dependencies of ROS-fireline configurations on fireline evolution requires further research. These dependencies could be important since each would change the intensity and therefore in-draft needs of head or flanking section of a fire.

Ideally, numerical investigations such as those described here or those into additional sensitivities would be performed in concert with new observation and experimental data to validate the numerical results or test hypotheses described in this text. A key requirement to validation of the phenomena suggested by these numerical results is that comparative observations and experiments be designed and instrumented at sufficient spatial and temporal resolution to describe not only the fire behavior, but also the dynamic and spatially homogeneous environmental conditions. The model results presented here, suggest that coupled atmospheric and wildfire dynamics are driven by a range of intricately balanced processes that occur across a spectrum of length and time scales. The value of numerical modeling for improving understanding of the complexities of fire behavior is greatly enhanced by complementary experiments or observations that can test model driven hypotheses, provide validation data for model results or pose new details of phenomenology for comprehensive numerical investigation.

Acknowledgements

We thank Kevin Heirs and the Joseph W. Jones Ecological Research Center at Ichauway in addition to Caroline Sieg and the Rocky Mountain Research Station, USDA Forest Service for funding this research via resources from the National Fire Plan. All computations were performed through the Los Alamos National Laboratory Institutional Computing Center (LANL ICN). Simulated fire visualizations were created using ParaView visualization software, maintained by Kitware. Many thanks go to LANL ICN and Kitware for the resources and support provided for this work. We also thank Philip Cunningham for many valuable discussions into the details of vorticity and the role that it plays in wildfire behavior.

References

- Asai, T., 1970. Stability of a plane parallel flow with variable vertical shear and unstable stratification. *Journal of the Meteorological Society of Japan* 48 (2), 129–139.
- Baines, P.G., 1990. Physical mechanisms for the propagation of surface fires. *Mathematical and Computational Modeling* 13, 83–94.
- Beer, T., 1991. The interaction of wind and fire. *Boundary-Layer Meteorology* 54, 287–308.
- Beer, T., 1993. The speed of a fire front and its dependence on wind speed. *International Journal of Wildland Fire* 3, 193–202.
- Carrier, G.F., Fendell, F.E., Wolff, M.F., 1991. Wind-aided fire spread across arrays of discrete fuel elements. I. Theory. *Combustion Science and Technology* 75, 31–51.
- Catchpole, W.R., Catchpole, E.A., Butler, B.W., Rothermel, R.C., Morris, G.A., Latham, D.J., 1998. Rate of spread of free-burning fires in woody fuels in a wind tunnel. *Combustion Science and Technology* 131, 1–37.
- Cheney, N.P., Gould, J.S., Catchpole, W.R., 1993. The influence of fuel, weather and fire shape variables on fire-spread in grasslands. *International Journal of Wildland Fire* 3, 31–44.
- Cheney, N.P., Gould, J.S., 1995. Fire growth in grassland fuels. *International Journal of Wildland Fire* 5, 237–244.
- Cheney, N.P., Gould, J.S., Catchpole, W.R., 1998. Prediction of fire spread in grasslands. *International Journal of Wildland Fire* 8, 1–13.
- Clever, R.M., Busse, F.H., 1991. Three-dimensional convection in a horizontal fluid layer subjected to a constant shear. *Journal of Fluid Mechanics* 229, 517–529.
- Clever, R.M., Busse, F.H., 1992. Three-dimensional convection in a horizontal fluid layer subjected to a constant shear. *Journal of Fluid Mechanics* 234, 511–527.
- Cunningham, P., Linn, R.R., 2007. Numerical simulations of grass fires using a coupled atmosphere–fire model: dynamics of fire spread. *Journal of Geophysical Research* 112 (D5).
- Deardorff, J.W., 1965. Gravitational instability between horizontal plates with shear. *Physics of Fluids* 8 (6), 1027–1030.
- Dupuy, J.L., Larini, M., 1999. Fire spread through a porous forest fuel bed: a radiative and convective model including fire-induced flow effects. *International Journal of Wildland Fire* 9, 155–172.
- Dupuy, J.L., Marechal, J., Portier, D., Valette, J.-C., 2011. The effects of slope and fuel bed width on laboratory fire behavior. *International Journal of Wildland Fire* 20, 272–288.
- Finney, M.A., 1998. FARSITE: Fire Area Simulator – Model Development and Evaluation. Research Paper RMRS-RP-4. USDA Forest Service, Ogden, Utah.
- Finney, M.A., Forthofer, J., Grenfell, I.C., Adam, B.A., Akafuah, N.K., Saito, K., 2013. A study of flame spread in engineered cardboard fuelbeds. Part I. Correlations and observations of flame spread. In: Seventh International Symposium on Scale Modeling, Hirosaki, Japan, August 2013.
- Floryan, J.M., 1991. On the Gortler instability in boundary layers. *Progress in Aerospace Sciences* 28, 235–271.
- Fons, W.L., 1946. Analysis of fire spread in light forest fuels. *Journal of Agricultural Research* 72 (3), 93–121.
- Gage, K.S., Reid, W.H., 1968. The stability of thermally stratified plane Poiseuille flow. *Journal of Fluid Mechanics* 33 (1), 21–32.
- Grishin, A.M., 1997. Mathematical Modeling of Forest Fires and New Methods of Fighting Them. Publishing House of the Tomsk State University.
- Kiefer, M.T., Parker, M.D., Charney, J.J., 2009. Regimes of dry convection above wild-fires: idealized numerical simulations and dimensional analysis. *Journal of the Atmospheric Sciences* 66, 806–836.
- Kiefer, M.T., Parker, M.D., Charney, J.J., 2010. Regimes of dry convection above wild-fires: sensitivity to fireline details. *Journal of the Atmospheric Sciences* 67, 611–632.
- Koo, E., Pagni, P., Woycheese, J., Stephens, S., Weise, D., Huff, J., 1997. A simple physical model for forest fire spread rate. In: *Fire Safety Science: Proceedings of the Eighth International Symposium*, pp. 851–862.
- Kuo, H.L., 1963. Perturbations of plane Couette flow in stratified fluid and origin of cloud streets. *Physics of Fluids* 6 (2), 195–211.
- Larini, M., Giroud, F., Porterie, B., Loraud, J.-C., 1998. A multiphase formulation for fire propagation in heterogeneous combustible media. *International Journal of Heat and Mass Transfer* 41 (6), 881–897.
- Linn, R.R., 1997. A transport model for the prediction of wildfire behavior. Los Alamos National Laboratory, Los Alamos, NM (dissertation) LA-13334-T, 195 pp.
- Linn, R.R., Harlow, F.H., 1998. Mixing-limited transport model used for description of wildfires. In: *Computational Technologies for Fluid/Thermal/Structural/Chemical Systems with Industrial Applications*. ASME, New York, pp. 161–168.
- Linn, R.R., Cunningham, P., 2005. Numerical simulations of grass fires using a coupled atmosphere–fire model: basic fire behavior and dependence on wind speed. *Journal of Geophysical Research* 110 (D13).
- Linn, R.R., Canfield, J.M., Cunningham, P., Edminster, C., Dupuy, J.-L., Pimont, F., 2012. Using periodic line fires to gain a new perspective on multi-dimensional aspects of forward fire spread. *Agriculture and Forest Meteorology* 157, 60–76.
- Margerit, J., Séro-Guillaume, O., 2002. Modeling forest fires. Part II. Reduction to two-dimensional models and simulation of propagation. *International Journal of Heat and Mass Transfer* 45, 1723–1737.
- Maughan, J., Incropera, F., 1987. Secondary flow in horizontal channels heated from below. *Experiments in Fluids* 5 (5), 334–343.
- Mell, W., Jenkins, M.A., Gould, J., Cheney, P., 2007. A physics-based approach to modeling grassland fires. *International Journal of Wildland Fire* 16, 1–22.
- Morvan, D., Dupuy, J.L., 2001. Modeling of fire spread through a forest fuel bed using a multiphase formulation. *Combustion and Flame* 127 (1), 1981–1994.
- Pagni, P.J., Peterson, T.G., 1973. Flame spread through porous fuels. *Symposium (International) on Combustion* 14 (1), 1099–1107.
- Reisner, J.M., Wynn, S., Margolin, L., Linn, R.R., 2000. Coupled atmospheric-fire modeling employing the method of averages. *Monthly Weather Review* 128, 2683–3691.
- Rothermel, R.C., 1972. A Mathematical Model for Predicting Fire Spread in Wildland Fuels. USFS.
- Séro-Guillaume, O., Margerit, J., 2002. Modeling forest fires. Part I. A complete set of equations derived by extended irreversible thermodynamics. *International Journal of Heat and Mass Transfer* 45, 1705–1722.
- Sparrow, E., Husar, R., 1969. Longitudinal vortices in natural convection flow on inclined plates. *Journal of Fluid Mechanics* 37, 251–255.
- Weise, D.R., (PhD thesis) 1993. Modeling wind and slope-induced wildland fire behavior. University of California, Berkeley.
- Wolff, M.F., Carrier, G.F., Fendell, F.E., 1991. Wind-aided fire spread across arrays of discrete fuel elements. II. Experiment. *Combustion Science and Technology* 77, 261–289.
- Zhou, X., Mahalingam, S., Weise, D., 2005. Modeling of marginal burning state of fire spread in live chaparral shrub fuel bed. *Combustion and Flame* 143 (3), 183–198.